doi:10.2533/chimia.2012.208 Chimia 66 (2012) 208–211 

# Dynamical Processes in Rydberg-Stark Deceleration and Trapping of Atoms and Molecules

Christian Seiler[§], Stephen D. Hogan, and Frédéric Merkt*

[§]SCS-Metrohm Foundation Award for best oral presentation

*Abstract:* The interaction between inhomogeneous electric fields and the large electric dipole moments of atoms and molecules in Rydberg states of high principal quantum number can be used to efficiently accelerate and decelerate atoms and molecules in the gas phase. We describe here how hydrogen atoms and molecules initially moving with velocities of ~600 m/s in supersonic beams can be decelerated to zero velocity and loaded into electric traps. The long observation times that are made possible by the electrostatic trapping enables one to study slow relaxation processes. Experiments are presented in which we have observed photoionization processes and transitions between Rydberg states induced by blackbody radiation at temperatures between 10 K and 300 K on a time scale of several milliseconds. Comparison of these processes in Rydberg states of H and $H_2$ suggests the importance, in $H_2$, of collisional processes and of the process of blackbody-radiation-induced predissociation.

**Keywords:** Blackbody radiation · Cold molecules · Rydberg states · Stark deceleration

## 1. Introduction

High Rydberg states are electronically excited states of atoms and molecules that consist of a positively charged ion core weakly interacting with a distant electron excited to an orbital of high principal quantum number $n$.[1,2] Their energy is well described by the Rydberg formula

$$\frac{E_{n,\ell}}{hc} = \frac{E_{\rm I}}{hc} - \frac{\rm Ry}{(n-\delta_\ell)^2} \qquad (1)$$

where $E_{\rm I}$ is the ionization energy, Ry the mass-dependent Rydberg constant and $\delta_l$, the quantum defect of states with angular momentum quantum number $l$. $\delta_l$ is typically zero for non-penetrating states ($l$>3, in small molecules). The physical properties of the electron–ion-core system scale with integer powers of the principal quantum number. For instance, the binding energy scales as $1/n^2$, the lifetime as $n^3$, the size of the Rydberg orbital as $n^2$ and the dipole moment as $n^2$. These scaling laws are such that Rydberg states with $n$>20 have unusual properties. These properties can be exploited in a variety of scientific and technological applications[3] such as high-resolution photoelectron spectroscopy,[4] photofragment translational spectroscopy[5] and electric-field sensing.[6]

Recently, and following an early proposal by Breeden and Metcalf,[7] the large dipole moments of high Rydberg states have been exploited to deflect,[8] slow down,[9,10] reflect[11] and trap beams of Rydberg atoms and molecules, and load them at low translational temperatures into electric traps.[12–15] Combined with the long lifetimes of Rydberg states, the ability to store low-temperature samples of Rydberg atoms and molecules in traps enables one to study slow relaxation processes, such as radiative transitions induced by blackbody radiation[16] and slow predissociation, and to study interactions between Rydberg states and surfaces.[17–19] We describe here recent measurements of very slow relaxation processes in high Rydberg states of H atoms and $H_2$ molecules stored at translational temperatures of ~100 mK in electric traps following Rydberg-Stark deceleration.

## 2. Principles of Rydberg-Stark deceleration

The high electronic degeneracy of Rydberg states ($n^2$ for H atoms[20]) can be removed by the application of an external electric field, which results in a predominantly linear Stark effect. The levels split in $n$–|$m$| components ($m$ is the magnetic quantum number associated with the Rydberg-electron orbital motion), the splitting being linear at low fields, as depicted for the H atom in Fig. 1(a). The linear dependence of the energy shifts $\Delta W_{\rm Stark}$ on the field strength $F$ can be expressed as

$$\Delta W_{\rm Stark} = \frac{3}{2} a_0 e n k\, F \qquad (2)$$

where $a_0$ and $e$ are the Bohr radius and the elementary charge, respectively, and $k$ is an integer running from –$n$+|$m$|+1 to $n$–|$m$|–1 in steps of 2. The linear Stark shift corresponds to an electric dipole moment $\mu_{\rm el} = \frac{3}{2} a_0 e n k$. In an inhomogeneous electric field $\vec{F}$ with field strength $F(\vec{r})$ Rydberg atoms experience a force $\vec{f}$ given by

$$\vec{f} = -\nabla\left(E_{\rm pot}\right) = -\nabla\left(\Delta W_{\rm Stark}\right) = \frac{3}{2} a_0 e n k \nabla F\left(\vec{r}\right) \ . \qquad (3)$$

*Correspondence: Prof. Dr. F. Merkt
Laboratory of Physical Chemistry
ETH Zürich
Wolfgang-Pauli-Str. 10
CH-8093 Zürich
Tel.: +41 44 632 43 67
Fax: +41 44 632 10 21
E-mail: feme@xuv.phys.chem.ethz.ch

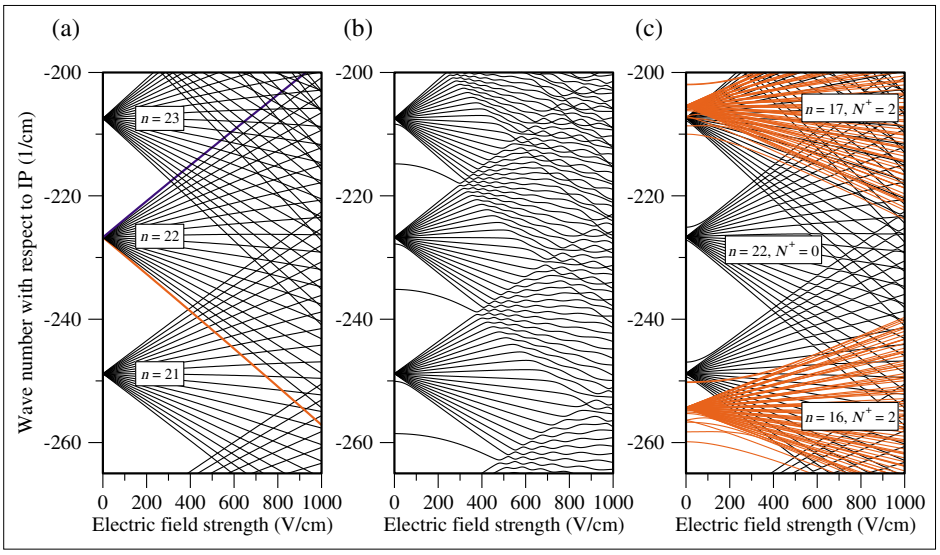


Fig. 1. (a) Calculated $|m|$=0 Stark map for the hydrogen atom. Shown in blue (red) is the Rydberg-Stark state of the $n$=22 manifold with the most positive (negative) electric dipole moment. (b) Calculated $|m|$=0 Stark map for the lithium atom in the vicinity $n$=21-23. (c) Calculated $|M_J|$=0 Stark map for para $H_2$ including series converging to the ground $N^+$=0 ($n$=21-23, shown in black) and first excited $N^+$=2 ($n$=16-17, shown in red) rotational levels.

The outermost Stark states in Fig. 1(a) correspond to states with $\mu_{el} \approx \frac{3}{2} a_0 e n^2$ (3430 Debye at $n$ = 30). Field gradients of $10^8$ V/m$^2$ are easily produced in the laboratory resulting in accelerations of $7\times10^8$ m/s$^2$ for hydrogen Rydberg atoms at $n$=30. Deceleration and trapping experiments on Rydberg atoms and molecules rely on these very large accelerations. The experiments are typically carried out with states exhibiting a positive Stark shift. Indeed, it is possible to generate three-dimensional inhomogeneous electric-field distributions with a minimum, but not a maximum in space, and the forces resulting from Eqn. (3) for states of positive $k$ value always direct the Rydberg atoms or molecules towards regions of lower electric-field strength.

Fig. 1 also depicts the Stark effect in a non-hydrogenic atom, lithium, in panel (b), and in a molecule, $H_2$, in panel (c). The Stark effect in these systems is similar to that of H with two exceptions: The penetrating low-$l$ states have a non-zero quantum defect, and the crossings between different Stark states are exact in H but avoided in non-hydrogenic systems. However, any non-hydrogenic system can be made hydrogenic by excluding penetrating low-$l$ components from the Rydberg-electron wavefunction. This is achieved by preparing states with $|m|\geq3$, *e.g.* using multiphoton excitation with circularly polarized radiation from the ground state, as explained in detail in ref. [21]. The experiments presented in the next sections are carried out with such hydrogenic states.

In these experiments, inhomogeneous electric fields are generated by applying time-dependent potentials to suitably designed metallic components referred to as electrodes (see Fig. 2(c) for an example). In the electrode design, one seeks to optimize the field gradients (and thus the forces according to Eqn. (3)). One then adjusts the time dependence of the potentials so that the field gradients remain large, and the field remains approximately constant throughout the acceleration/deceleration and trapping processes (see ref. [16] for details).

A schematic view of our Rydberg-Stark decelerator is presented in Fig. 2(a). Translationally and internally cold atomic and molecular samples are produced in a supersonic expansion into vacuum from a high pressure reservoir behind a nozzle. The supersonic beam is collimated by a skimmer and enters a region where the atoms are excited to a specific Rydberg state with narrow-band lasers and then decelerated and trapped using time-dependent inhomogeneous electric fields.[12,13]

We use the ten-electrode decelerator shown in Fig. 2(b). This decelerator enables us to either trap the atoms or molecules between electrodes labelled 1–4 along the supersonic-beam propagation axis, or off-axis between electrodes 2, 4, 7 and 8. This off-axis trapping[16] permits us to avoid losses of particles from the trap caused by collisions with atoms and molecules in the trailing edge of the gas beam. The entire deceleration and trapping region is surrounded by concentric heat shields and can be cooled to ~10 K to study the effects of blackbody-radiation-induced transitions.

The field distribution in the on-axis and off-axis traps, corresponding to voltages of +12 V applied to electrodes 1, 4 and 7 and –12 V applied to electrodes 2, 3 and 8, are depicted in Fig. 2(c). The traps are deep enough to confine atoms with kinetic energies below $k_BT$ on the order of 1 K. The electrodes labeled 5 (6) and 9 (10) in Fig. 2(b) are located above (below) the plane

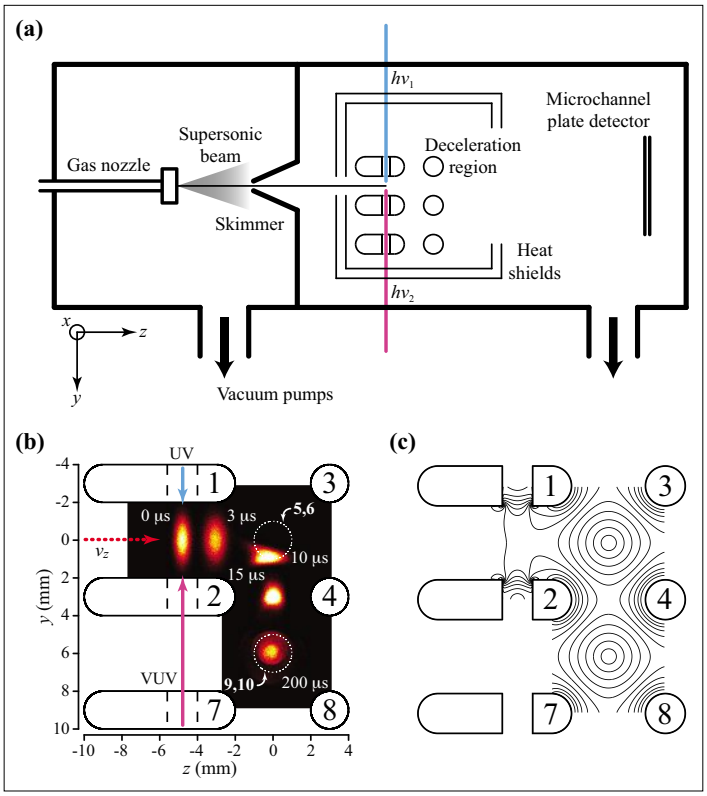


Fig. 2. (a) Schematic diagram of the experimental setup used to decelerate and trap translationally cold Rydberg atoms and molecules. (b) Schematic diagram of the Rydberg-Stark deceleration, deflection and trapping device with simulated snapshots of a $n$=30, $k$=19 Rydberg H atom cloud at the time of photoexcitation ($t$ = 0 µs) and at times 2, 10, 15 and 200 µs. The electrodes are numbered 1–10 and electrodes 5 (6) and 9 (10) are located above (below) the plane of the figure. (c) Electrode setup in the $yz$ plane at the time of photoexcitation and after completion of the trapping process. The lines of constant electric fields range from 10 to 100 V/cm in steps of 10 V/cm.

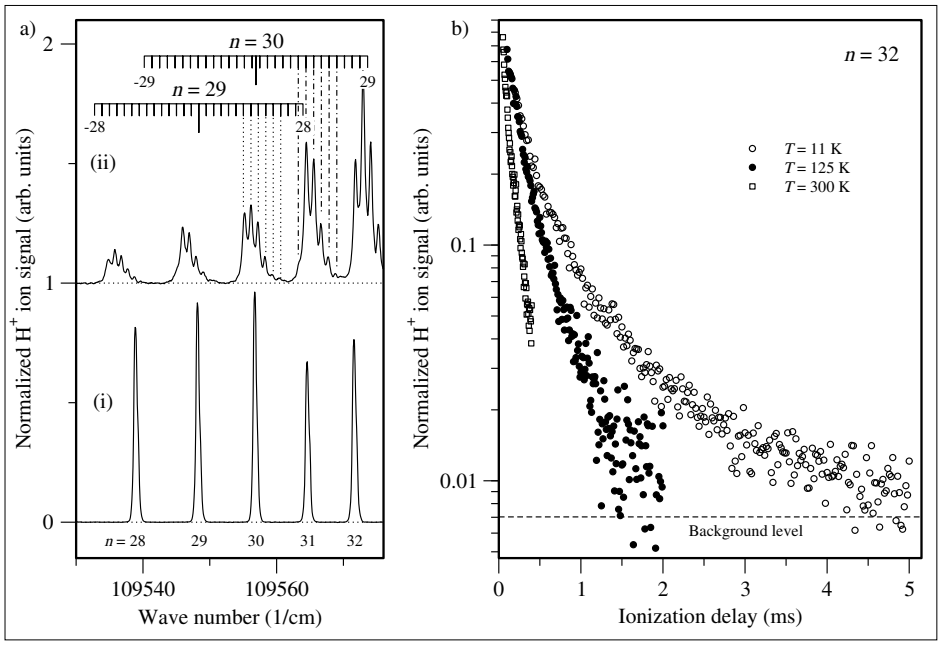


Fig. 3. (a),(i) $n$=28-32 Rydberg states recorded at zero electric-field strength. (ii) Spectrum of the electrostatically trapped low-field-seeking Stark states of H detected at $t_{ion}$ = 250 μs. (b) Measurement of the decay of H atoms from the off-axis trap initially excited to $n$=32 Rydberg states at electrode temperatures of 11 K (open circles), 125 K (full circles) and 300 K (open squares).

of the figure and are used to confine the particles along the $x$ dimension.

The Rydberg atoms and molecules are detected by pulsed electric field ionization. To this end, large positive voltage pulses are applied to electrodes 1, 2 and 7. The resulting electric-field pulses also extract the positively charged ions toward a micro-channel-plate detector. By monitoring the total field-ionization signal as a function of time delay between the field-ionization pulse and the laser excitation, it is possible to monitor the decay of the Rydberg atoms from the trap. Under our experimental conditions, this decay is the result of radiative and non-radiative processes changing the internal state of the Rydberg atoms or molecules.

## 3. Experiments with Trapped H Rydberg Atoms

In our experiments on H atoms, the atoms are produced by 193 nm excimer-laser photolysis of $NH_3$ in a capillary mounted at the exit of the pulsed valve.[22] The H atoms in the supersonic beam move with an initial velocity of 600 m/s. The deceleration and trap-loading process takes approximately 20 μs. Fig. 3(a) shows which Stark states are optimal for deceleration and trapping. Trace (i) displays a spectrum obtained by field ionization of the H atoms with $n$ in the range 28–32 immediately after laser excitation under field-free conditions, and without deceleration and trapping. Trace (ii) shows a spectrum recorded in the same spectral region, but following excitation in an electric field of 300 V/cm and subsequent deceleration and trapping for 250 μs. The spectrum consists of six blue-shifted Stark states at each $n$ value, with $k$ values in the range 11–21 at $n$=30. The positions of the other Stark states for $n$=29 and 30 at the electric field applied during laser excitation are indicated along the horizontal tab above the figure. This experiment shows that the trapping procedure selects atoms with dipole moments in the range 1260–2430 Debye.

Fig. 3(b) shows the results of measurements of the decay of the H atoms from the off-axis trap recorded at three different temperatures (300 K, 125 K and 11 K) of the electrodes and heat shield in a semi-log plot. These temperatures correspond to the blackbody-radiation temperature and not to the translational temperature (~100 mK) of the trapped samples. The decay at 300 K is approximately exponential with a 1/e-time of 105 μs. The decay is much slower at lower temperatures and reveals a multi-exponential behavior. At 125 K and 11 K, the initial part of the decay (up to $t$≤500 μs) can be approximately described by a 1/e-time of 220 μs and 225 μs, respectively.

These measurements illustrate the effect of blackbody radiation on the Rydberg atoms. At 300 K, a substantial fraction of the blackbody photons has a wave number larger than 100 $cm^{-1}$ which is sufficient to ionize the Rydberg atoms (The binding energy of an $n$=30 Rydberg electron is ~100 $cm^{-1}$). The measured decay time is found to be caused by spontaneous emission to the ground state and by blackbody-radiation-induced ionization, the latter process being the dominant one. At 125 K, the Planck distribution peaks at a wave number of ~400 $cm^{-1}$ and the intensity of the blackbody radiation is much weaker so that the importance of blackbody-radiation-induced photoionization is strongly reduced. The early decay is dominated by fluorescence to the ground state. However, transitions to neighbouring Rydberg states of similar dipole moments induced by the blackbody-radiation field leads to a gradual evolution of the population from the initially prepared Stark state to Stark states of neighbouring $n$ values. Because of the rapid scaling of the lifetime and the state density with $n$, the overall effect is a preferential population of higher $n$ states which have longer lifetimes at long trapping times. The rate of decay of the trapped-atom signal thus slows down with time. At 11 K, the experimental observation can be explained by the same arguments, but at these temperatures blackbody-radiation-induced ionization is completely negligible. Modeling the radiative processes leading to the observed trap decay enables one to quantitatively account for the observed trap losses.[16] The observation of the state redistribution induced by blackbody radiation, even at the lowest temperatures, enables us to conclude that the effects of blackbody radiation must be included in the analysis of other experiments, such as H atom photofragment translational spectroscopic experiments and experiments on antihydrogen at CERN.[23,24]

## 4. Experiments with Trapped $H_2$ Rydberg Molecules

When trapping Rydberg molecules, care has to be taken to exclude Stark states with penetrating (low-$l$) character, to avoid the non-hydrogenic behaviour depicted in Fig. 1(c) and to reduce losses by predissociation.[21] In our experiments on $H_2$, this is achieved by producing the Rydberg states in a resonant three-photon excitation with circularly polarized radiation. Starting from the $M_J$=0, $J$=0 ground state of $H_2$, $|M_J|$=3 Rydberg states are produced, for which $l$=0-2 components are absent from the Rydberg-electron wavefunction. The spectrum of $H_2$ is therefore hydrogenic, as illustrated by the two spectra displayed in Fig. 4(a) which are identical in appearance to those shown for H in Fig. 3(a). Another advantage of using non-penetrating molecular Rydberg states is that decay processes such as predissociation are strongly suppressed. The measurement of the decay of the molecules from the trap presented in Fig. 4(b) reveals much faster processes (1/e-time of 20 μs) than in the case of the H atom. The origin of the much faster decay cannot be attributed to spontaneous

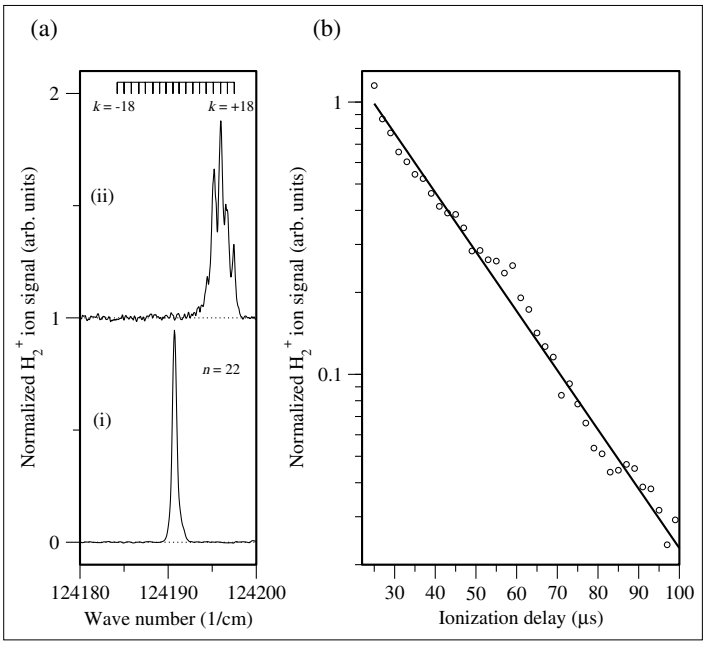


Fig. 4. (a),(i) $n$=22 Rydberg state recorded at zero electric-field strength. (ii) Spectrum of the electrostatically trapped low-field-seeking $n$=22, $k$=10-18, $|M_J|$=3 Stark states of $H_2$ detected at $t_{ion}$=50 μs with pulsed potentials of 1.7 kV applied for deceleration. (b) Semi-log plot of the measured (open circles) and fitted (full line) decay from the trap of $H_2$ molecules initially excited to $n$=33 Rydberg states.

emission because $|M_J|$=3 Rydberg states can only decay to levels with $n\leq 2$. The transitions to $n$=2 levels are in the near UV and the Einstein coefficients for spontaneous emission are reduced by a factor of more than 64 compared to emission to the ground state.

Up to now, we could only perform these measurements on $H_2$ at a blackbody temperature of 300 K. Because we do not observe a significant $n$ dependence of the trap decay times, we do not expect predissociation of the initially populated $|M_J|$=3 levels to be dominant. A possible explanation for the observed behavior is blackbody-radiation-induced predissociation. Indeed, the absorption of a low-frequency photon could induce transitions to Rydberg states of neighbouring $n$ values but with $|M_J|$=2 which could predissociate more rapidly because of the increased penetrating character of the Rydberg electron wavefunction. An alternative explanation is that the different decay times are caused by collisions. Experiments at lower blackbody-radiation temperatures and following trapping in the on- and off-axis traps are underway to clarify these processes.

### *Acknowledgments*

This work is supported financially by the Swiss National Science Foundation under Project 200020-132688 and by the European Research Council advanced grant program under Project 228286.

Received: February 13, 2012

[1] T. F. Gallagher, 'Rydberg Atoms', Cambridge University Press, Cambridge, **1994**.
[2] F. Merkt, *Ann. Rev. Phys. Chem.* **1997**, *48*, 675.
[3] F. Merkt, *Chimia* **2000**, *54*, 89.
[4] K. Müller-Dethlefs, E. W. Schlag, *Ann. Rev. Phys. Chem.* **1991**, *42*, 109.
[5] M. N. R. Ashfold, G. A. King, M. G. D. Nix, T. A. A. Oliver, in 'Handbook of High-resolution Spectroscopy', Eds. M. Quack, F. Merkt, John Wiley & Sons, Chichester, **2011**.
[6] A. Osterwalder, F. Merkt, *Phys. Rev. Lett.* **1999**, *82*, 1831.
[7] T. Breeden, H. Metcalf, *Phys. Rev. Lett.* **1981**, *47*, 1726.
[8] D. Townsend, A. L. Goodgame, S. R. Procter, S. R. Mackenzie, T. P. Softley, *J. Phys. B: At. Mol. Opt. Phys.* **2003**, *34*, 439.
[9] S. R. Procter, Y. Yamakita, F. Merkt, T. P. Softley, *Chem. Phys. Lett.* **2003**, *374*, 667.
[10] E. Vliegen, H. J. Wörner, T. P. Softley, F. Merkt, *Phys. Rev. Lett.* **2004**, *92*, 033005.
[11] E. Vliegen, F. Merkt, *Phys. Rev. Lett.* **2006**, *97*, 033002.
[12] E. Vliegen, S. D. Hogan, H. Schmutz, F. Merkt, *Phys. Rev. A* **2007**, *76*, 023405.
[13] S. D. Hogan, F. Merkt, *Phys. Rev. Lett.* **2008**, *100*, 043001.
[14] S. D. Hogan, C. Seiler, F. Merkt, *Phys. Rev. Lett.* **2009**, *103*, 123001.
[15] S. D. Hogan, P. Allmendinger, H. Saßmannshausen, H. Schmutz, F. Merkt, *Phys. Rev. Lett.* **2012**, *108*, 063008.
[16] C. Seiler, S. D. Hogan, H. Schmutz, J. A. Agner, F. Merkt, *Phys. Rev. Lett.* **2011**, *106*, 073003.
[17] E. So, M. Dethlefsen, M. Ford, T. P. Softley, *Phys. Rev. Lett.* **2011**, *107*, 093201.
[18] Y. Pu, D. D. Neufeld, F. B. Dunning, *Phys. Rev. A* **2010**, *81*, 042904.
[19] S. D. Hogan, J. A. Agner, F. Merkt, T. Thiele, S. Filipp, A. Wallraff, *Phys. Rev. Lett.* **2012**, *108*, 063004.
[20] H. A. Bethe, E. E. Salpeter, 'Quantum Mechanics of One- and Two-Electron Atoms', Springer, Berlin, **1957**.
[21] C. Seiler, S. D. Hogan, F. Merkt, *Phys. Chem. Chem. Phys.* **2011**, *13*, 19000.
[22] S. Willitsch, J. M. Dyke, F. Merkt, *Helv. Chim. Acta* **2003**, *86*, 1152.
[23] G. B. Andresen *et al., Nature Physics* **2011**, *7*, 558.
[24] A. Kellerbauer *et al., Nucl. Instr. and Meth. in Phys. Res. B* **2008**, *266*, 351.